DATA-DRIVEN ON-LINE PREDICTION OF THE AVAILABLE RECOVERY TIME IN NUCLEAR POWER PLANT FAILURE SCENARIOS

Enrico Zio, Francesco Di Maio

DATA-DRIVEN ON-LINE PREDICTION OF THE AVAILABLE RECOVERY TIME IN NUCLEAR POWER PLANT FAILURE SCENARIOS

Enrico Zio, Francesco Di Maio

Energy Department, Polytechnic of Milan
Via Ponzio 34/3, 20133 Milano, Italy
enrico.zio@polimi.it

ABSTRACT

This paper presents a data-driven approach for predicting the available Recovery Time (RT) of a system during a failure scenario, i.e., the time remaining until the system can no longer perform its function in an irreversible manner. A library of reference multidimensional trajectory patterns from failure scenarios is created. When a new failure scenario develops, its evolution pattern is compared by fuzzy similarity analysis to the reference multidimensional trajectory patterns. The time remaining before the developing trajectory pattern hits a failure threshold is predicted by combining the times of failure of the reference patterns, weighed by their similarity to the developing pattern.

For illustration purposes, a case study of literature is considered regarding the estimation of the available RT in failure scenarios of the Lead Bismuth Eutectic eXperimental Accelerator Driven System (LBE-XADS).

Key Words: Recovery Time, Emergency Accident Management, Nuclear Power Plant, Lead-Bismuth Eutectic eXperimental Accelerator Driven System (LBE-XADS), Fuzzy Similarity Analysis, Pattern Recognition.

1. Introduction

Nuclear Power Plant (NPP) Accident management involves the anticipation of paths of potentially dangerous behaviors, the prediction of the related effects and actions to avoid any undesired impact on the safety of the NPP [IAEA, 2003].

In case of an accident, or an initiating event that may develop into an accident, the plant personnel must perform various tasks before taking counteracting actions:

- Identification of the plant state: this diagnostic task aims at identifying the cause of the problem and the states of a number of parameters critical for the plant operation and safety;
- Prediction of the future development of the accident: this involves prediction of the future evolution of the states of the critical parameters and correspondingly of the behavior of the plant and its residual Recovery Time (RT) , i.e., the time available for corrective actions before system failure;
- Planning of accident mitigation strategies, to be activated if safe control of the accident evolution were not successful.

In modern accident management, computers and computerized procedures are useful tools which aid operators in the tasks of obtaining reliable information, following procedures, identifying plant states, predicting the future accident progression and planning accident control and mitigation actions. In particular, the complicated phenomena that take place in a NPP during an accident situation are more accessible to computerized handling than to human expert evaluation [Øwre, 2001]. Yet, the problem of what kind of decision support to provide to nuclear power plant operators, in particular during transients leading up to accidents, is far from trivial [NEA, 1992; EC 1999; USNRC, 1999; IAEA, 2003].

Fortunately, NPP personnel have the capability to effectively manage a broad range of accidents; their successful management of complex accident behaviors requires that they detect the occurrence of the accident, determine the extent of challenge to plant safety, monitor the performance of active, passive, automatic and digital systems, select strategies to prevent or mitigate the safety challenge, implement the action strategies, and monitor their effectiveness. The capability to effectively carry out these tasks during an accident is influenced by the availability of timely and accurate plant status information and the awareness of the RT after the detection of the fault. Poor decisions may be taken because of an assumed short time available for sorting out the information relevant to the plant status [Glasstone et al., 1998]; on the contrary, timely and correct decisions can prevent an event from developing into a severe accident or mitigate its undesired consequences.

The existing computer-based tools which can aid accident management can be categorized according to their complexity and specific application purpose [IAEA, 2003]:

- Compact simulators;
- Plant analyzers;
- Full-scope training simulators;
- Multifunctional simulators;
- Severe accident simulators;
- Accident management support tools.

In particular, the accident management support tools combine tracking and predictive simulators. The former ones monitor the plant status and provide calculated values also of those parameters that are not directly observable by the monitoring systems. The predictive simulators must be fast-running so as to allow on-line prediction of the accident progression and of the effects of the planned mitigation strategies [IAEA, 2003].

The critical point of predictive simulators is the speed of computation, to provide real time information. This of course depends on the level of detail included in the plant modeling and on the computer power available.

One of the main quantities of interest to be delivered by predictive simulators for accident management use is the available RT. Approaches to RT prediction can be categorized broadly into model-based and data-driven [Chiang et al., 2001]. Model-based approaches attempt to incorporate physical models of the system into the estimation of the RT. However, uncertainty due to the assumptions and simplifications of the adopted models may pose significant limitations. Moreover, the requirement of high computational speed for on line response necessarily leads to limited details in the phenomena modeled, with consequent limited accuracy in the representation of the actual plant behavior [Berglund et al., 1995; Serrano et al., 1999]. On the contrary, data-driven techniques utilize monitored operational data related to system health. They can be beneficial when understanding of first principles of system operation is not straightforward or when the system is so complex that developing an accurate model is prohibitively expensive. Data-driven approaches can often be deployed quickly and cheaply, and still provide wide coverage of system behavior. An added value of data-driven techniques is their ability to transform high-dimensional noisy data into lower dimensional information useful for decision-making [Dragomir et al., 2007].

Data-driven approaches can be divided into two categories: statistical techniques (regression methods, ARMA models, etc.) and Artificial Intelligence (AI) techniques (neural networks, fuzzy logic systems, etc.).

With respect to AI techniques, Neural Networks (NNs) and Fuzzy Logic (FL) techniques have gained considerable attention in the past few years, due to their ability to deal with the uncertainties and non-linearities of the real processes, especially in abnormal conditions [Øwre, 2001]. Successful prediction models have been constructed based on Neural Networks [Barlett et al., 1992; Campolucci et al., 1999; Peel et al., 2008; Zio et al., 2008; Santosh et al., 2009] and Neuro-Fuzzy (NF) systems [Wang et al., 2004]. In spite of the recognized power of neural network modeling techniques, skepticism against their use in safety-critical applications relates to their black-box character which limits intuition with respect to the understanding of their performance [Wang et al., 2008].

An opportunity for increased transparency and openness of data-driven models is offered by fuzzy logic methods, which are increasingly proposed in modern control and diagnostic technologies. Based on the principles of Zadeh's fuzzy set theory, fuzzy logic provides a formal mathematical framework for dealing with the vagueness of everyday reasoning [Zadeh, 1965]. As opposed to binary reasoning based on ordinary set theory, within the fuzzy logic framework measurement uncertainty and estimation imprecision can be properly accommodated [Yuan et al., 1997; Zio et al., 2005].

The goal of this work is to extend to the multidimensional case an approach previously presented by the authors for the prediction of the available RT during an accident [Zio et al., 2009]. The extension is necessary for dealing with realistic cases of accident management. The multidimensional computational framework for the on-line prediction of the system available RT considers a set of multidimensional trajectory patterns arising from different system failures (hereafter called reference trajectory patterns) and uses a fuzzy-based, data-driven similarity analysis for predicting the RT of a newly developing failure trajectory (hereafter called test trajectory pattern). A novelty of the proposed computational framework lies in the reliance on a fuzzy definition of multidimensional trajectory pattern similarity to capture and integrate the ambiguous information carried by the measured signals. More specifically, the pattern matching process is based on a fuzzy evaluation of the distance between the signals of the multidimensional test pattern and the patterns of reference [Angstenberger, 2001]; the fuzzy distances from all reference patterns are then combined to transform the multidimensional data into a one-dimensional similarity indicator, which is used in the prediction of the available RT.

An application is presented with reference to the dynamic failure scenarios of the Lead Bismuth Eutectic eXperimental Accelerator Driven System (LBE-XADS) with digital Instrumentation and Control (I&C) [Cammi et al., 2006]. Keeping the focus on RT prediction, the analysis does not cover the study of the software and its possible failure modes, the benefits of fault tolerant features, the interactions of the software with the hardware and human components. In other words, the dynamic failure scenario modeling is tailored to the purpose of showing the feasibility of effectively estimating the RT during an accident. The actual implementation of the method in a qualified tool of accident management will require full dynamic accident calculations, inclusive of comprehensive models of hardware, software and human failure modes and their interactions.

The paper is structured as follows. Section 2 provides a detailed description of the computational algorithm for the multidimensional fuzzy data similarity evaluation and the associated RT prediction. Section 3 presents the mechanistic model of the LBE-XADS, with the description of the monitored signals. In Section 4, the results of the application of the approach to LBE-XADS failure scenarios are presented. Finally, some conclusions are drawn in Section 5.

2. Methodology

It is assumed that *N* trajectories (reference trajectory patterns) are available, representative of the evolution of relevant signals during reference failure scenarios. These trajectories last all the way to system failure, i.e., to the time when anyone of the signals reaches the threshold value beyond which the system loses its functionality.

When a failure scenario is developing in the system, its multidimensional signal trajectory (test trajectory pattern) is compared for similarity with the *N* multidimensional reference trajectory patterns stored in the database and the residual lifes of these are used to estimate the RT available in the developing failure scenario [Angstenberger, 2001].

Figure 1 shows a schematics of the computational framework in the general case of multidimensional trajectories of *Z* monitored signals $f\left(x_1, x_2, ..., x_Z, t\right)$.

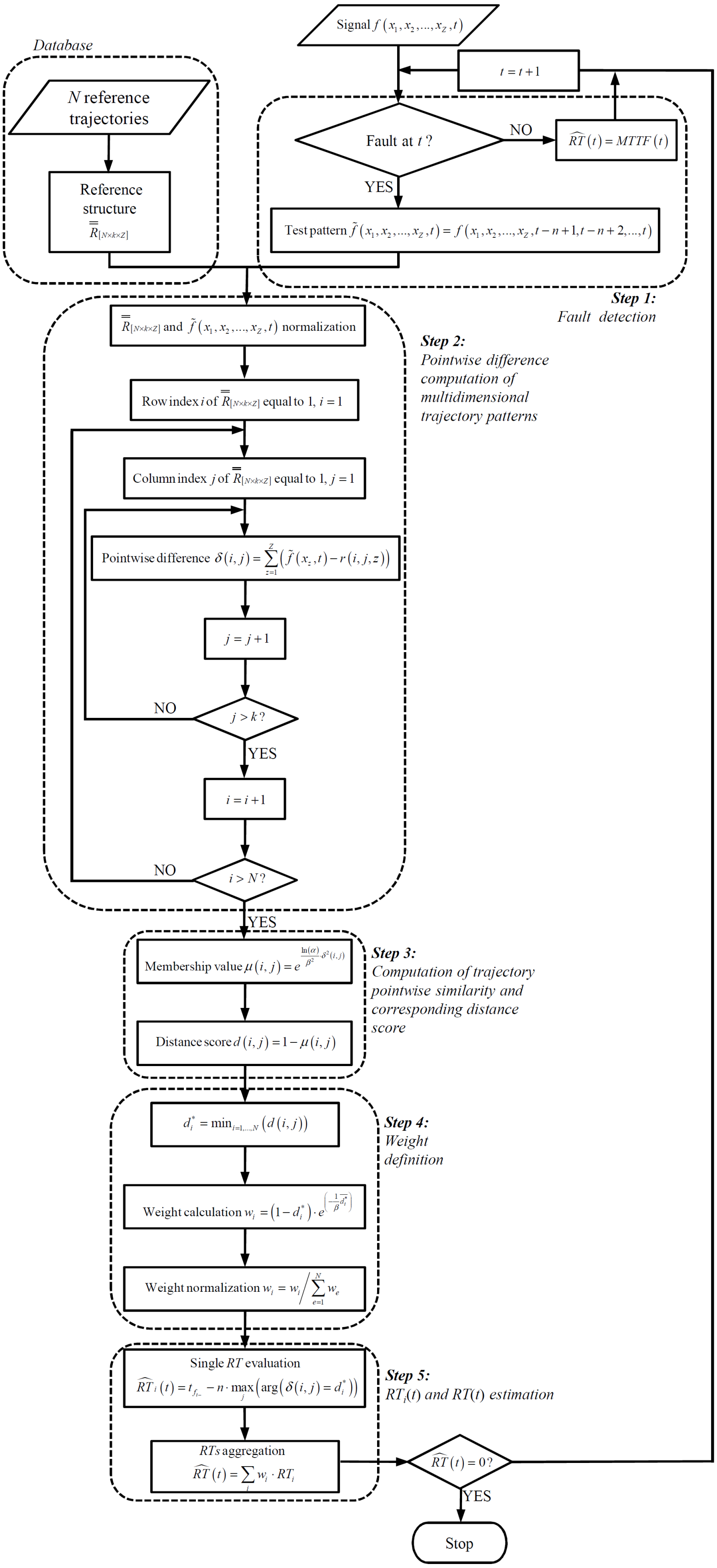

Figure 1 The flowchart of the fuzzy based data-driven approach

For illustration, the procedure is here followed step by step:

- ***Step 1***: ***fault detection***. The *Z*-dimensional trajectory of signals $f\left(x_1, x_2, ..., x_Z, t\right)$ is continuously monitored throughout the time horizon of observation T, starting from (discrete) time $t=1$; at each discrete time t, its values are recorded and appended to the matrix of the values collected at the previous time steps. For reasons which will become clear in the following, the database containing the reference trajectory patterns is organized in a 3-D structure $\overline{\overline{R}}_{[N\times k\times Z]}$, where $k=\frac{T}{n}$ and its generic element $r\left(i, j, z\right)$ is the projection on the *z*-th signal axis of $r\left(i, j\right)$ which is the *j*-th segment of length n of values of the *i*-th reference trajectory, $i=1,2,...,N$, $j=1,2,...,k$, $z=1,2,...,Z$, normalized in the range [0.2,0.8]. For clarity's sake, in Figures 2 and 3 a 2-D reference trajectory and its partition into 15 elements are shown, respectively (i.e., *Z*=2 and *k*=15). As long as no abnormal signal deviation is detected, the system is qualified as working in nominal conditions and the estimate $\widehat{RT}\left(t\right)$ of the available recovery time made at the generic time t is taken equal to the system Mean Time to Failure $MTTF\left(t\right)$, obtained from the available recovery time $RT_i\left(t\right)$ of all the failure trajectories in the reference library:

$$\widehat{RT}\left(t\right)=MTTF\left(t\right)=\frac{1}{\left(|\, i \,\|\, t_{f_i}>t\right)}\sum_{i|t_{f_i}>t}\left(t_{f_i}-t\right)=\frac{1}{\left(|\, i \,\|\, t_{f_i}>t\right)}\sum_{i|t_{f_i}>t}RT_i\left(t\right) \tag{1}$$

where t_{f_i} is the system failure time along the *i*-th trajectory (i.e., the time when the signal value exceeds the threshold beyond which the system loses its functionality), $\left(|\, i \,\|\, t_{f_i}>t\right)$ is the cardinality of the set of reference trajectories whose failure time is larger than t and $RT_i\left(t\right)$ is their residual life starting from t. At the following time steps, the algorithm continues to update the estimate of $\widehat{RT}(t) = MTTF(t)$, until a fault is detected upon a deviation of the signal outside its range of allowed variability; at this time, the algorithm for the estimation of the available RT starts matching the similarity of the developing signal trajectory evolution to those in the reference library, and combining their failure times to provide an estimate of the available RT.

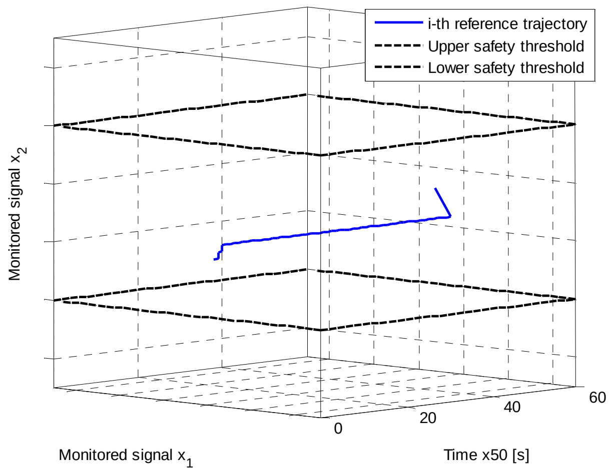

Figure 2 A bidimensional reference trajectory on a time horizon *T*=3000 [s]

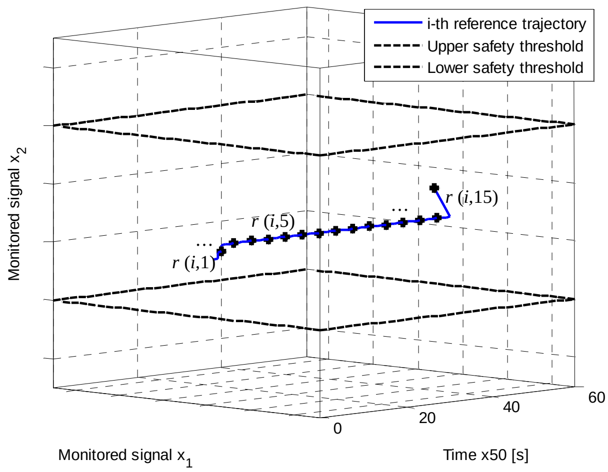

Figure 3 Bidimensional reference trajectory of Figure 2 partitioned into *k*=15 segments of length *n*=3000/15=200 [s], *j*=1,2,…,15

- ***Step 2*: *pointwise difference computation of multidimensional trajectory patterns*.** At the current time *t*, the latest *n*-long segment of values of the test trajectory pattern $\tilde{f}(x_1, x_2, ..., x_Z, t) = f(x_1, x_2, ..., x_Z, t-n+1, t-n+2, ..., t)$ is normalized in [0.2,0.8]. The pointwise difference $\delta(\bullet)$ between the $n \cdot Z$ values of pattern $\tilde{f}(x_1, x_2, ..., x_Z, t)$ and those of the generic reference trajectory segment $r(i, j, z)$, is computed:

$$\delta(i, j) = \sum_{z=1}^{Z} \left(\tilde{f}(x_z, t) - r(i, j, z) \right), \; i = 1, 2, ..., N, \; j = 1, 2, ..., k, \; z = 1, 2, ..., Z \tag{2}$$

The matrix $\overline{\overline{\delta}}_{[N\times k]}$ contains the difference measures $\delta(i,j)$ between all n-long segments of the Z-dimensional reference trajectories and the test trajectory pattern of the monitored signals.

- ***Step 3***: ***computation of trajectory pointwise similarity and corresponding distance score***. Classically, similarity is decided crisply: depending on whether the distance or similarity measure between two objects exceeds a specified threshold, the objects are classified into distinct categories of 'similar' or 'non-similar' [Angstenberger, 2001]. Such binary classification is restrictive when the situation is not so clear-cut and imprecision and uncertainty in similarity classification exist [Zimmermann et al., 1985]. In practice, there are numerous cases in which the similarity measure should allow for a gradual transition between 'similar' and 'non-similar' [Binaghi et al., 1993; Joentgen et al., 1999]. This can be achieved by resorting to a fuzzy logic modeling paradigm in which the pointwise difference of two trajectories is judged for similarity with respect to an "approximately zero" fuzzy set (FS) specified by a function which maps the elements $\delta(i,j)$ of the difference matrix $\overline{\overline{\delta}}_{[N\times k]}$ into their values $\mu(i,j)$ of membership to the condition of "approximately zero". The distance score $d(i,j)$ between two trajectory segments is then computed as:

$$d(i,j)=1-\mu(i,j),\ i=1,2,...,N\ ,\ \ j=1,2,...,k \tag{3}$$

Common membership functions can be used for the definition of the FS, e.g. triangular, trapezoidal, and bell-shaped [Dubois et al., 1988]. In the application illustrated in this work, the following bell-shaped function is used:

$$\mu(i,j)=e^{-\left(\frac{-\ln(\alpha)}{\beta^2}\delta^2(i,j)\right)} \tag{4}$$

The arbitrary parameters α and β can be set by the analyst to shape the desired interpretation of similarity into the fuzzy set: the larger the value of the ratio $\frac{-\ln(\alpha)}{\beta^2}$, the narrower the fuzzy set and the stronger the definition of similarity [Zio et al., 2009]. The choice of the values of α and β depends on the application; one may proceed to determining the value β of the difference value δ which must have a degree of membership μ equal to α [Angstenberger, 2001]

- ***Step 4***: ***weight definition***. The $\widehat{RT}(t)$ is estimated as a similarity-weighted sum of the $RT_i(t)$:

$$\widehat{RT}(t) = \sum_{i \mid t_{f_i} > t} w_i \cdot RT_i(t), \; i = 1, 2, ..., N \tag{5}$$

The ideas behind the weighting of the individual $RT_i(t)$ is that: *i*) all failure trajectories in the reference library bring useful information for determining the available RT of the trajectory currently developing; *ii*) those segments of the reference trajectories which are most similar to the most recent segment of length n of the currently developing failure trajectory should be more informative in the extrapolation of the occurring trajectory to failure.

To assign the weight w_i, the minimum distance d_i^* along the i^{th} row of the matrix of Eq. (3) is first identified:

$$d_i^* = \min_{j=1,...,k} d(i, j), \; i = 1, 2, ..., N \tag{6}$$

The weight w_i is then computed as:

$$w_i = \left(1 - d_i^*\right) \cdot e^{\left(-\frac{1}{\beta} d_i^*\right)} \ , \ i = 1, 2, ..., N \tag{7}$$

and normalized:

$$w_i = w_i \Big/ \sum_{e=1}^{N} w_e \tag{8}$$

Note that the smaller the minimum distance the larger the weight given to the *i*-th trajectory [Zio et al., 2009].

- ***Step 5*: *RT***

for which $t_{f_i} > t$, the value $RT_i\left(t\right)$ is determined as:

$$RT_i\left(t\right) = t_{f_i} - t_{j_M} \ , \ i = 1, 2, ..., N \tag{9}$$

where $t_{j_M} = n \cdot \max_j \left(\arg\left(\delta\left(i, j\right) = d_i^*\right)\right)$ is the final time index of the latest-in-life segment of the *i*-th trajectory among those with minimum distance d_i^* from the developing test trajectory (*n* is the test trajectory pattern length and $\max_j \left(\arg\left(\delta\left(i, j\right) = d_i^*\right)\right)$ gives the largest column index *j* of $r\left(i, \bullet\right)$ whose element is equal to d_i^*). Thus, $RT_i\left(t\right)$ is the time available before reaching the failure threshold on the reference trajectory starting from the end time of the latest-in-life segment of minimum distance from the developing trajectory (Figure 4).

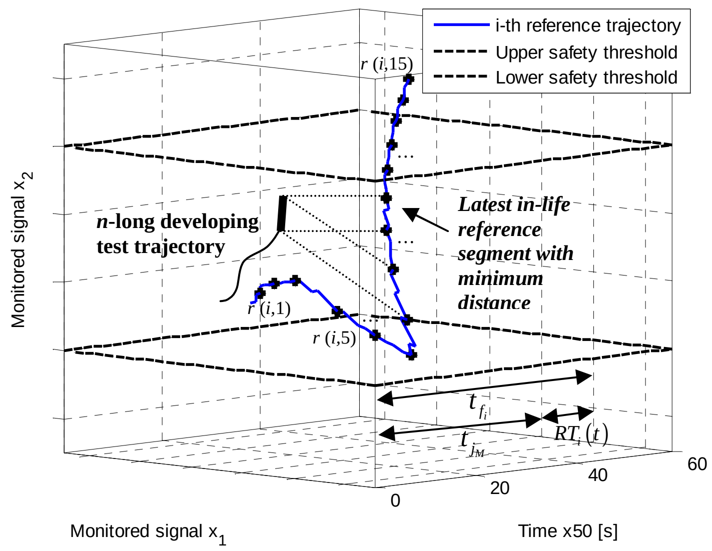

Figure 4 The $RT_i(t)$ for the *i*-th bidimensional reference trajectory starts from the end time of the latest-in-life segment of minimum distance from the occurring trajectory

This allows a conservative RT estimation, biased towards “pessimistic” predictions of the available RT, because in the case that more than one segment along the *i*-th reference trajectory is closest to the developing test trajectory, the latest one is taken, i.e., the one closest to failure.

Then, the estimate $\widehat{RT}(t)$ of the remaining useful life along the developing trajectory is simply computed as in Eq. (5), with weights w_i evaluated by Eq. (8).

3. The LBE-XADS

The Lead-Bismuth Eutectic eXperimental Accelerator Driven System (LBE-XADS) is a sub-critical, fast reactor in which the fission process for providing thermal power $P(t)$ is sustained by an external neutron source through spallation reaction by a proton beam $Q(t)$ accelerated by a synchrotron on a lead-bismuth eutectic target [Bowman et al., 1992; Carminati et al., 1993; Rubbia et al., 1995; Van Tuyle et al., 1993; Venneri et al., 1993]. A simplified scheme of the plant is sketched in Figure 5. The primary cooling system is of pool-type with Lead-Bismuth Eutectic

(LBE) liquid metal coolant leaving the top of the core, at full power nominal conditions, at temperature $\tau_{LB}^{C,P}$ equal to 400 °C and then re-entering the core from the bottom through the down-comer at temperature $\tau_{LB}^{P,C}$ equal to 300 °C. The average in-core temperature of the LBE $T_{LB}^{av,C}$ is taken as the mean of $\tau_{LB}^{C,P}$ and $\tau_{LB}^{P,C}$. The secondary cooling system is a flow of an organic diathermic oil at 290-320 °C, at full power conditions. Cooling of the diathermic oil in each loop is obtained through an air flow $\Gamma_a(t)$ provided by three air coolers connected in series.

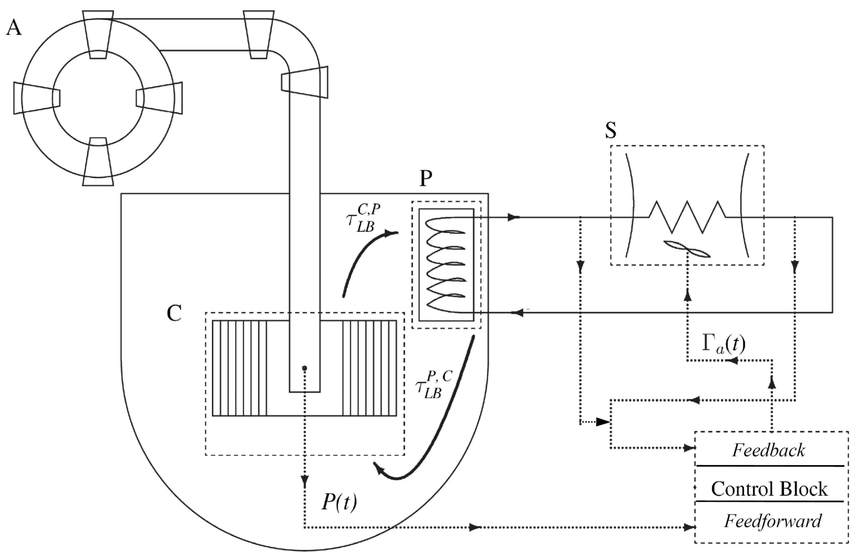

Figure 5 LBE-XADS simplified schematics. A = Accelerator; C = core; P = primary heat exchanger; S = secondary heat exchanger

A dedicated, dynamic simulation model has been implemented in SIMULINK for providing a simplified, lumped and zero-dimensional description of the coupled neutronic and thermo-hydraulic evolution of the system [Cammi et al., 2006]. The model allows the simulation of the system controlled dynamics as well as of the free dynamics when the control module is deactivated and the air cooler flow is kept constant.

Both feedforward and feedback digital control schemes have been adopted for the operation of the system. The control is set to keep a steady state value of approximately 300 °C of the average temperature of the diathermic oil $T_o^{av,S}$: this value represents the optimal working point of the diathermic oil at the steady state, full nominal power of 80 MWth. On the contrary, an oil temperature beyond the upper threshold $T_o^{th,u}$ =340 °C would lead to degradation of its physical and chemical properties, whereas a temperature below the lower threshold $T_o^{th,l}$ =280 °C could result in thermal shocks for the primary fluid and, eventually, for the structural components [Cammi et al., 2006]. Conservatively, no dependence on the duration of exposition to temperatures beyond the threshold values has been assumed: in other words, the system is considered to fail at such temperatures regardless of the time during which it exceeds the thresholds.

Multiple component failures can occur during the system life. To simulate this, the model has been embedded within a Monte Carlo (MC) sampling procedure for injecting faults at random times and of random magnitudes. Samples of component failures are drawn within a mission time of 3000 [s]. The set of faults considered are:

- The PID controller fails stuck, with a random flow rate output value m_1 sampled from a uniform distribution in [0,797] [kg/s].
- The air coolers fail stuck in a random position that provides a corresponding air flow mass m_2 uniformly distributed in [0,1000] [kg/s].
- The feedforward controller fails stuck with a corresponding flow rate value m_3 uniformly distributed in [0,797] [kg/s].
- The communication between air coolers actuators and PID controller fails so that the PID is provided with the same input value of the previous time step.

The first three faults are applicable to both analog and digital systems, whereas the last one is typical of digital systems. Furthermore, the fault magnitude probability distributions are assumed to be uniform, even if the components may more likely fail in a certain mode than in others. This includes also rare multiple events in the set of failure scenarios and further tests the robustness of the RT prediction procedure.

The sequence of multiple failures is generated by sampling the first failure time from the uniform distribution [0,3000] [s] and the successive failure times from the conditional distributions, uniform from the last sampled time to 3000 [s]. This assumption is conservative, favoring larger number of failures in the sequence.

The evolution of the failure scenarios may lead to three different end states, within the mission time of 3000 [s]:

1. Low-temperature failure mode ($T_o^{av,S} < T_o^{th,l}$)
2. Safe mode ($T_o^{th,l} < T_o^{av,S} < T_o^{th,u}$)
3. High-temperature failure mode ($T_o^{av,S} > T_o^{th,u}$)

The following three signals are taken for the estimation of the available RT:

- Mean in-core LBE temperature, $T_{LB}^{av,C}$
- Mean oil temperature of the secondary heat exchanger hot side , $T_o^{av,S}$
- Mean air flow rate at the secondary heat exchanger cold side, $\Gamma_a(t)$

It is important to underline that the procedure implemented in this work for sampling the fault events is not intended to reproduce the actual stochastic failure behavior of the system components; rather, the choices and hypotheses for modeling the faults (i.e., the mission time, the number and typology of faults, the distributions of failure times and magnitudes) have been arbitrarily made with the aim of favoring multiple failures. In any case, the components considered subjected to fault and their types are not intended to provide a comprehensive description of the system fault behavior but are only taken as exemplary for generating the dynamic failure scenarios to be used as reference and test patterns.

4. Results

4.1 Application of the procedure for RT(t) prediction

A database of Z=3-dimensional reference trajectories (i.e., $T_{LB}^{av,C}$, $T_{o}^{av,S}$ and $\Gamma_a(t)$) for N = 6400 failure scenarios (differing in faulty components, time of faults occurrence and faults magnitude) is organized in the reference structure $\overset{=}{R}_{[N\times k\times Z]}$, where $k=\frac{T}{n}$=30. The generic element $r(i,j,z)$ of the reference structure will be compared for similarity with the z-th signal of the test trajectory pattern containing the values of the latest 100 time steps of the trajectory. For each of the test trajectories the procedural steps are performed as follows:

Step 1: ***fault detection.***

The signal $f(x_1,x_2,x_3,t)$ is monitored starting from time $t=1$ [s] to the mission time T = 3000 [s], with time steps of 1 [s]. At each time step t, its value is appended and stored in the matrix containing the $n-1$=99 values of the 3 signals collected at the previous times. The Mean Time to Failure $MTTF(t)$ is calculated resorting to Eq. (1) and $\widehat{RT}(t)$ is set equal to $MTTF(t)$ for each time step, until any component failure is detected; the fault detection activates the on-line fuzzy-based data-driven algorithm for RT prediction.

Step 2: pointwise difference computation of multidimensional trajectory patterns.

The total pointwise difference $\delta(i,j)$ is evaluated by resorting to Eq. (2), with z=1,2,3.

Step 3: ***computation of trajectory pointwise similarity and corresponding distance score***.

The pointwise differences $\delta(i,j)$ are mapped into values of membership $\mu(i,j)$ of the "approximately zero" FS. The bell-shaped function of Eq. (4) is taken with parameters values $\alpha=0.2$ and $\beta=0.01$, implying strong sharpness in the FS and thus in the similarity requirement. The distance scores $d(i,j)$ are then computed by Eq. (3), $i=1,2,...,6400$, $j=1,2,...,30$.

Step 4: weight definition.

The minimum distances d_i^* are evaluated (Eq. (6)), and the relative normalized weights w_i calculated through Eqs. (7) and (8), $i = 1, 2, ..., 6400$.

Step 5*: *RTi(t) and RT(t) estimation.

For each reference trajectory in the library, an estimate $\widehat{RT}_i(t)$ for the test trajectory is computed (Eq. (9), $i = 1, 2, ..., 6400$); then, the $RT_i(t)$ are aggregated in the weighted sum (Eq. (5)) with the weights w_i previously calculated.

The estimates of the $MTTF(t)$ for five 3-D test pattern trajectories taken from [Zio et al., 2009] are plotted in Figures 6-10, in thin continuous lines with the bars of one standard deviation of the samples $\left(t_{f_i} - t \,|\, t_{f_i} > t\right)$, where t_{f_i} is the time at which the diathermic oil temperature profile of the *i*-th reference trajectory exceeds either thresholds $T_o^{th,u}$ or $T_o^{th,l}$, with corresponding system loss of functionality. The $\widehat{RT}(t)$ estimates obtained based on trajectory segments of $n = 100$ [s] are plotted in bold circles; at the beginning of the test trajectories, the predictions match the $MTTF(t)$; then, once a component failure is detected, the $\widehat{RT}(t)$ estimate moves away from the $MTTF(t)$ values towards the real *RT*(*t*) (dashed thick line). In the Figures, the bold vertical line indicates the time of diathermic oil threshold exceedance. Notice that none of the estimates exceeds the actual failure time.

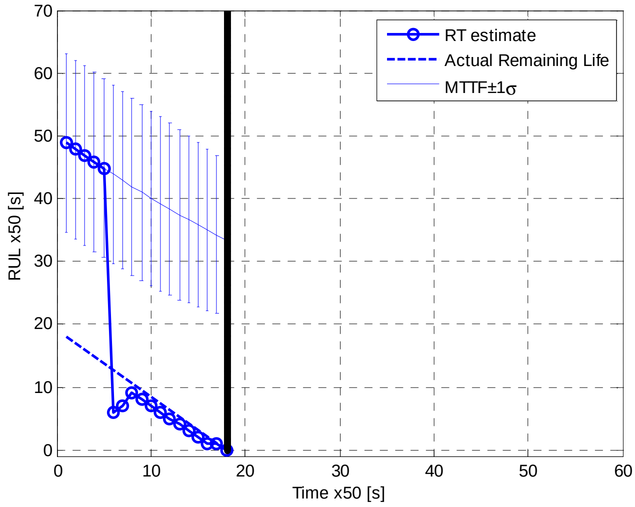

Figure 6 RT estimation for a trajectory belonging to the low-temperature failure mode

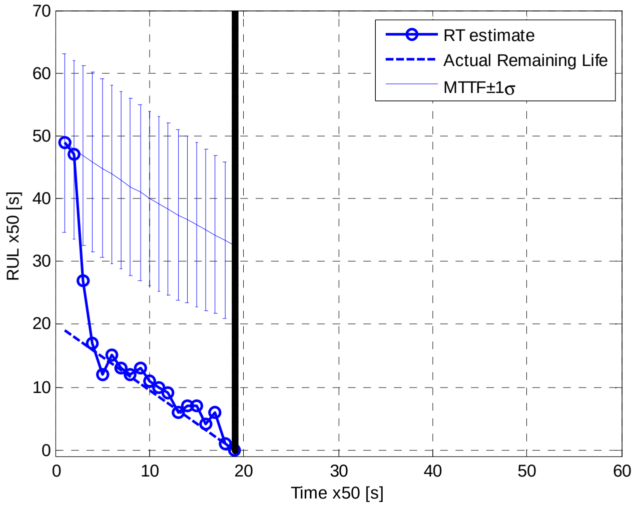

Figure 8 RT estimation for a trajectory belonging to the high-temperature failure mode

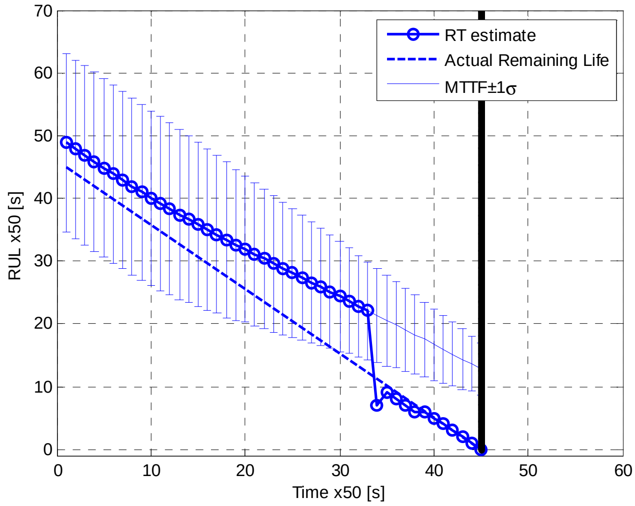

Figure 7 RT estimation for a trajectory belonging to the low-temperature failure mode

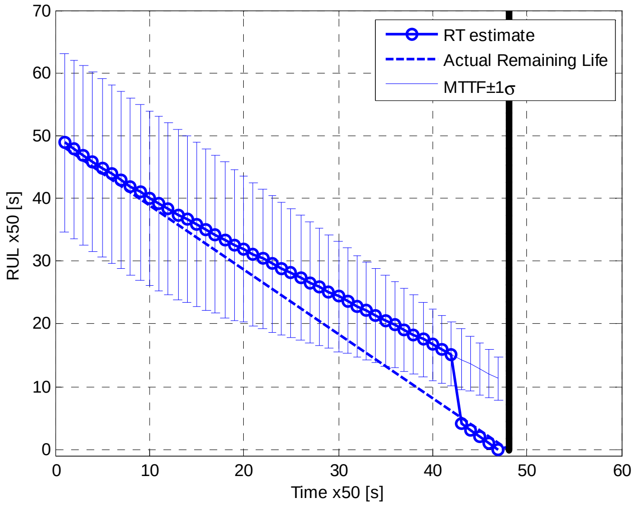

Figure 9 RT estimation for a trajectory belonging to the high-temperature failure mode

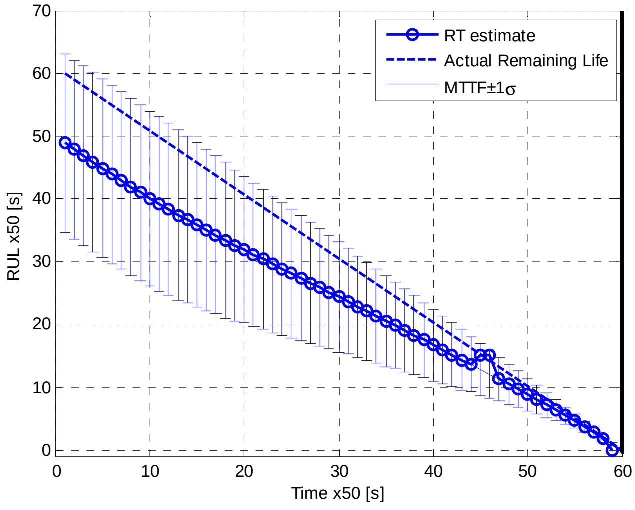

Figure 10 RT estimation for a trajectory which does not exceed any safety threshold value, although a failure sequence has occurred

4.2 Performance evaluation of the RT(t) estimation procedure

The performance of the available RT estimation procedure has been tested extensively on a batch of P=1280 multidimensional test trajectories, different from the reference trajectories. Figure 11 shows the $\widehat{RT}(t)$ predictions (continuous line with dark bullets) compared to the actual remaining lives for 25 failure trajectories (graphically appended in sequence), after the fault has been detected (i.e., starting from step 2 of the algorithm). After fault detection, the initial predictions for each test trajectory tend to be similar, regardless of the eventual length of the test trajectory life duration because the initial deviation from the nominal evolution is little sensitive and only slightly moves the $RT(t)$ prediction away from the $MTTF(t)$ value; this results in a conservative trend of initial anticipation of the available RT associated to trajectories whose failure actually occurs late in life. The largest available RT estimation errors occur for those trajectories in which the component failure is of low-magnitude, whose effect only slowly drives the system to failure and the prediction away from $MTTF(t)$ towards the true $RT(t)$.

To globally quantify the performance of the procedure, the mean relative error (RE) at time t, between the estimate $\widehat{RT}(t)$ and its true value $RT(t)$, is introduced:

$$RE(t) = \frac{1}{P}\sum_{p=1}^{P}\frac{\left|\widehat{RT}_p(t) - RT_p(t)\right|}{RT_p(t)} \tag{10}$$

where $RT_p(t)$ is the actual available recovery time at time t of test pattern p, and $\widehat{RT}_p(t)$ its estimate, $p = 1, 2, \ldots, P$.

Figure 12 shows the empirical probability density function of the mean relative error evaluated along 3000 [s] of evolution of the 1280 test trajectories. The distribution is skewed towards small error values, with mean and median equal to 0.07 and 0.02, respectively. This proves that the procedure most frequently makes small relative estimation errors.

The computational time required for the estimation along one complete test trajectory of 3000 [s] is of few seconds on an Intel® Celeron M of 900 MHz.

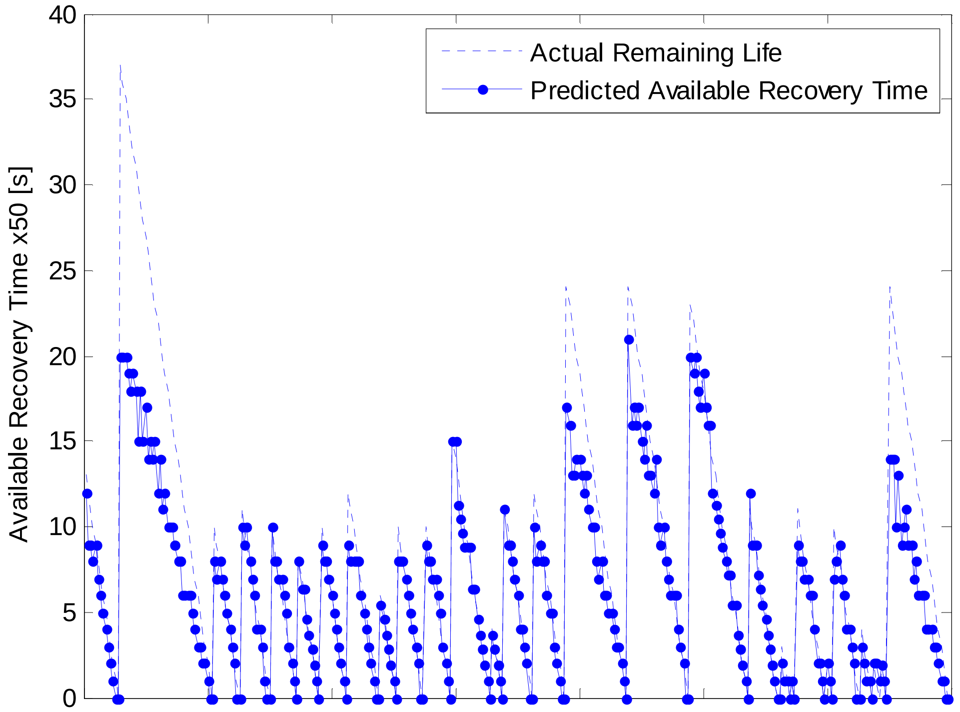

Figure 11 Predicted and actual remaining life for 25 test failure scenarios

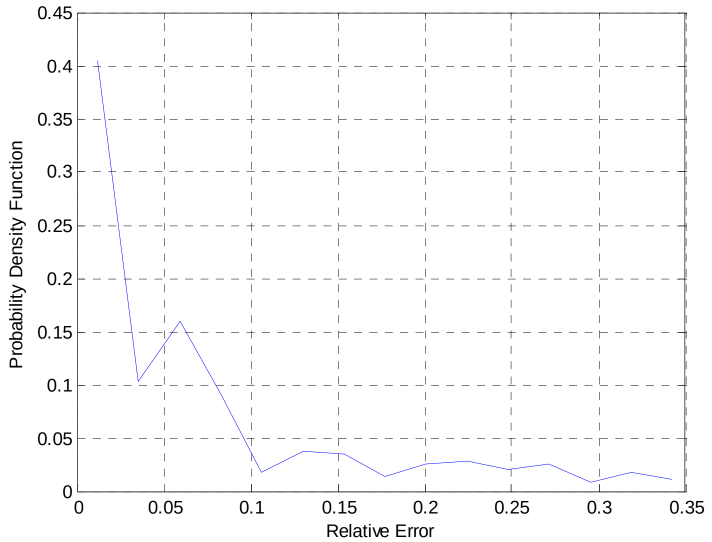

Figure 12 Empirical probability density function of the relative errors on the 3000 [s] of the 1280 test trajectories

Figure 13 compares the RE evaluated at time steps of 50 [s] in the last 600 [s] when all three monitored signals are used or when only the mean LBE temperature is used [Zio et al., 2009] with $\beta = 0.01$ in Eqs. (4) and (7). It is seen that:

- the accuracy in the estimation is worst when using only the mean LBE temperature;
- the accuracy in the estimation of the available RT improves over time: as the available RT decreases, the relative errors approximate their mean values of 0.02 and 0.05, respectively.
- the accuracy in the estimation of the available RT when all 3 monitored signals are used never exceeds a RE value of 0.1.

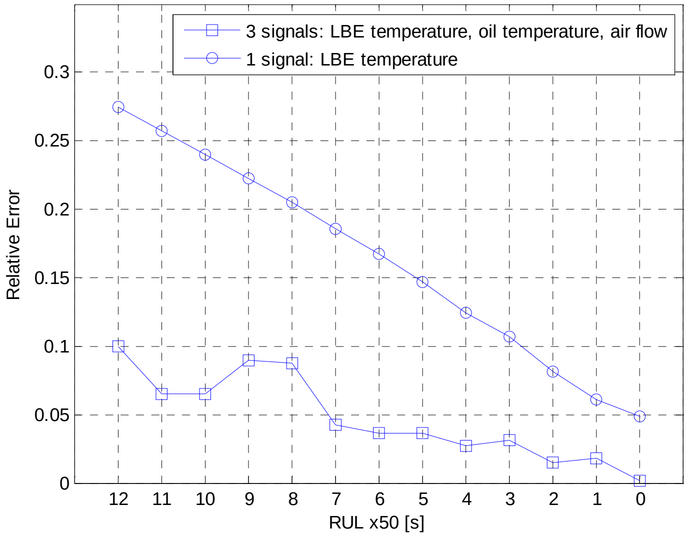

Figure 13 Relative Error evaluated each 50 [s] starting from 600 [s] before failure, for 1280 test trajectories, using all three monitored signals (squares) or only the mean LBE temperature (circles)

Figure 14 shows the RE evaluated at time steps of 50 [s] in the last 600 [s] for different groups of the three simultaneously monitored signals with $\beta = 0.01$ in Eqs. (4) and (7); the smaller number of monitored signals used for the pattern similarity evaluation, the worse the accuracy in the estimation of the available RT but the larger the savings in computing times. In the case of only 1 monitored signal, the performances for LBE temperature and oil temperature are almost the same; the performance for air flow signal is much worse than those for LBE and oil temperature, whose values evolving in time are a consequence of an overall contribution of the parameters t_1, t_2,

t_3, t_4, m_1 and m_2; on the contrary, after a failure directly affecting the air flow, since its value is stuck to m_3, this signal loses any physical meaning related to the system behavior without carrying any additional information for the RT prediction.

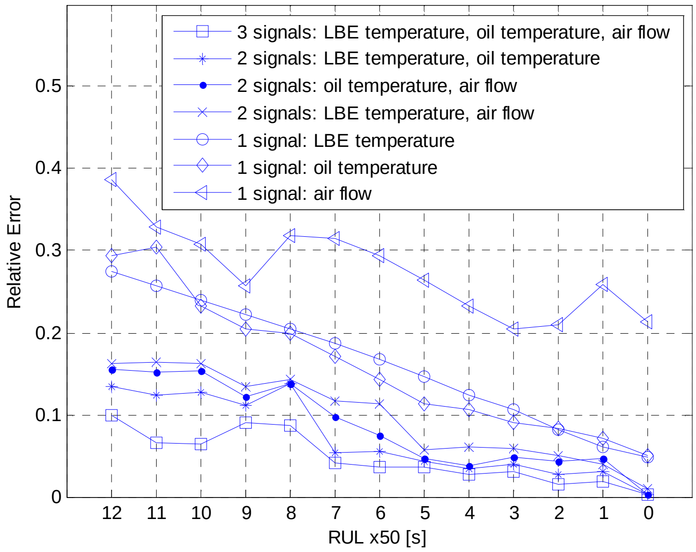

Figure 14 Relative Error evaluated each 50 [s] starting from 600 [s] before failure, for 1280 test trajectories, using different combinations of the three monitored signals

5. Conclusions

This paper extends to the multidimensional case a similarity-based prediction method for estimating the available Recovery Time (RT) of a system, as a computerized support tool to be embedded in an operator support system for emergency accident management. The capability of the staff to effectively carry out corrective actions is directly influenced by the availability of the information about the RT after the detection of the fault. In fact, poor decisions may be taken because of the supposed short time available for sorting out the relevant information; on the contrary, timely and correct decisions can prevent an event from developing into a severe accident or mitigate its undesired consequences.

The extended method of RT prediction allows for the consideration of the information carried out by multiple signals of multidimensional trajectories. Data from different transient failure scenarios are used to create a library of reference patterns of evolution; for estimating the available

RT of a test pattern, its evolution data are matched to the patterns in the library and their known residual life times are used for the estimation, based on a multidimensional fuzzy pointwise similarity concept.

The RT estimation procedure involves four main steps: (1) computing the pointwise difference between test and reference patterns; (2) evaluating their multidimensional fuzzy pointwise similarity and distance score; (3) defining the weights of the individual RT estimates provided by the reference patterns; and (4) aggregating these to evaluate the system residual RT.

A literature case study regarding the RT prediction for a large number of fault scenarios of the Lead Bismuth Eutectic eXperimental Accelerator Driven System (LBE-XADS) has demonstrated the promising potential of the computational procedure and the improvements in prediction accuracy obtained by extending it to multidimensional pattern analysis. The results are very satisfactory from the point of view of both accuracy of the estimation and computing time; these are two objectives which can be optimized by a proper selection of the monitored signals upon which to base the pointwise similarity evaluation. The procedure may be used to allow predicting the available RT with sufficient accuracy and timing for proactive maintenance/safety procedures purposes.

References

[Angstenberger, 2001] Angstenberger, L., Dynamic Fuzzy Pattern Recognition, International Series in Intelligent Technologies, 17, Kluwer Academic Publishers, 2001.

[Barlett et al., 1992] Barlett, E.B., Uhrig, R.E., Nuclear Power Plant Status Diagnostics Using an Artificial Neural Network, Nuclear Technology, 97, 1992.

[Binaghi et al., 1993] Binaghi, E., Della Ventura, A., Rampini, A., Schettini, R. (1993) Fuzzy Reasoning Approach to Similarity Evaluation in Image Analysis. International Journal of Intelligent Systems, Vol. 8, 1993, p. 749-769, 1993.

[Berglund et al., 1995] Berglund et.al, The use of CAMS during a safety exercise at the Swedish Nuclear Inspectorate, HWR-423. OECD Halden Reactor project –July 1995

[Bowman et al., 1992] Bowman, C.D., Arthur, E.D., Lisowski, P.W., Lawrence, G.P., Jensen, R.J., Anderson, J.L., Blind, B., Cappiello, M., Davidson, J.W., England, T.R., Engel, L.N., Haight, R.C., Hughes, H.G., Ireland, J.R., Krakowski, R.A., LaBauve, R.J., Letellier, B.C., Perry, R.T., Russell, G.J., Staudhammer, K.P., Versamis, G., Wilson, W.B., Nuclear energy generation and

waste transmutation using an accelerator-driven intense thermal neutron source. Nucl. Instr. Meth. Phys. Res. A 320, 336, 1992.
[Cammi et al., 2006] Cammi, A., Luzzi, L., Porta, A. A. and Ricotti, M. E., Modelling and control strategy of the Italian LBE-XADS, Progress in Nuclear Energy, Volume 48, Issue 6, Pages 578-589, 2006.
[Campolucci et al., 1999] Campolucci, P., Uncini, A., Piazza, F. and Rao, B.D., On-Line Learning Algorithms of Locally Recurrent Neural Networks, IEEE Trans. Neural Networks, 10, pp. 253-271, 1999.
[Carminati et al., 1993] Carminati, F., Klapisch, R., Revol, J.P., Roche, Ch., Rubio, J.A., Rubbia, C., An Energy Amplifier for Cleaner and Inexhaustible Nuclear Energy Production Driven by a Particle Beam Accelerator. CERN Report CERN-AT-93-47(ET), 1993.
[Chiang et al., 2001] Chiang L. H., Russel, E., Braatz R., Fault detection and diagnosis in industrial systems, Springer-Verlag, London, 2001.
[Dragomir et al., 2007] Dragomir, O.E., Gouriveau, R., Zerhouni, N., Dragomir, F., Framework for a Distributed and Hybrid Prognostic System, In 4th IFAC Conference on Management and Control of Production and Logistics, 2007.
[Dubois et al., 1988] Dubois, D., Prade, H., Testemale, C., Weighted Fuzzy Pattern Matching. Fuzzy Sets and Systems, 28, 1988, p. 313-331, 1988.
[EC, 1999] EC, EU research in Reactor safety: Achievements of the 4th and prospects for the 5Th Euratom framework programme. Eurocourse 1999. GRS, May 1999.
[Glasstone et al., 1998] Glasstone, S, Sesonske, A., Nuclear reactor engineering. New Delhi: CBS Publishers and Distributors; 1998.
[IAEA, 2003] IAEA, Application of simulation techniques for accident management training in nuclear power plants, ISBN: 9201039034, 2003
[Joentgen et al., 1999] Joentgen, A., Mikenina, L., Weber, R., Zimmermann, H.-J., Dynamic Fuzzy Data Analysis based on Similarity between Functions. Fuzzy Sets and Systems, 105 (1), 1999, p. 81-90, 1999.
[NEA, 1992] NEA, Severe Accident Management – Prevention and Mitigation., Paris, 1992
[Øwre, 2001] Øwre, F., Role of the man–machine interface in accident management strategies, Nuclear Engineering and Design 209, 201–210, 2001
[Peel et al., 2008] Peel, L., Data Driven Prognostics using a Kalman Filter Ensemble of Neural Network Models, International Conference on Prognostics and Health Management, 2008.
[Rubbia et al., 1995] Rubbia, C., Rubio, J.A., Buono, S., Carminati, F., Fitier, N., Galvez, J., Gels, C., Kadi, Y., Klapisch, R., Mandrillon, P., Revol, J.P., Roche, Ch., Conceptual Design of a Fast Neutron Operated High Power Energy Amplifier. CERN Report CERN-AT-95-44(ET), 1995.
[Santosh et al., 2009] Santosh, T.V., Srivastava, A., Sanyasi Rao, V.V.S., Gosh, A. K., Kushwaha, H.S., Diagnostic System for Identification of Accident Scenarios in Nuclear Power Plants using Artificial Neural Networks, Reliability Engineering and System Safety, 94, 759-762, 2009.
[Serrano et al., 1999] Serrano et al., Development of an extension of the CAMS system to severe accident management, HWR-580. OECD Halden Reactor project –May 1999
[USNRC, 1999] USNRC 1999, NUREG-0700, Rev.1 - Human-System Interface Design Review Guideline, USNRC, Washington, June 1996
[Van Tuyle et al., 1993] Van Tuyle, G.J., Todosow, M., Geiger, M.J., Aronson, A.L., Takahashi, H., Accelerator-driven subcritical target concept for transmutation of nuclear wastes. Nucl. Technol. 101, 1, 1993.
[Venneri et al., 1993] Venneri, F., Bowman, C.D., Jameson R., Accelerator-driven Transmutation of Waste (ATW) - A New Method for Reducing the Long-term Radioactivity of Commercial Nuclear Waste. Los Alamos Report LA-UR-93-752, 1993

[Wang et al., 2008] Wang T., Yu, J., Siegel, D., Lee, J., A similarity based prognostic approach for Remaining Useful life estimation of Engineered Systems, International Conference on Prognostics and Heath Management, 2008.
[Wang et al., 2004] Wang, W.Q., Goldnaraghi, M.F., Ismail, F., Prognosis of Machine Health Condition using Neuro-Fuzzy Systems, Mechanical Systems and Signal Processing, 18, 813-831, 2004.
[Yuan et al., 1997] Yuan, B., Klir, G., Data driven identification of key variables, In: Ruan, D. (Ed.), Intelligent Hybrid Systems Fuzzy Logic, Neural Network, and Genetic Algorithms. Kluver Academic Publishers, pp.161–187, 1997.
[Zimmermann et al., 1985] Zimmermann, H.-J., Zysno, P., Quantifying Vagueness in Decision Models. European Journal of Operational Research, Vol. 22, 1985, p. 148-158, 1985.
[Zadeh, 1965] Zadeh, L., Fuzzy sets, Inform. Control 8, 338–353, 1965.
[Zio et al., 2005] Zio, E., Baraldi, P., Identification of nuclear transients via optimized fuzzy clustering, Annals of Nuclear Energy, 32, 1068–1080, 2005.
[Zio et al., 2008] Zio, E., Pedroni, N., Broggi, M., Golea, L., Locally recurrent neural networks for nuclear dynamics modeling, FLINS - The 8th International FLINS Conference on Computational Intelligence in Decision and Control, 21-24 September 2008, Madrid, Spain, 2008.
[Zio et al., 2009] Zio, E., Di Maio, F., A Data Driven Fuzzy Approach for predicting the Remaining recovery Time in a Dynamic Fault Scenarios of a Nuclear System, under review, Reliability Engineering and System Safety, 2009.